

Case Report

J Vet Intern Med 2017;31:142–148**Pyogranulomatous Pancarditis with Intramyocardial *Bartonella henselae* San Antonio 2 (*BhSA2*) in a Dog**

T.A. Donovan, P.R. Fox, N. Balakrishnan, M. Ericson, V. Hooker, and E.B. Breitschwerdt

Key words: Canine; Myocarditis; Nephritis; Stealth; Vasculitis.**Case History and Findings**

A 6-year-old, female, spayed American Pitbull terrier was presented for progressive lethargy, weakness, and anorexia of 3-weeks duration. The dog was found as a stray in New York City (NYC) approximately 4 years earlier, assessed to be 2 years of age, and in very poor condition. Pertinent past medical history included a deep hindquarter wound and minor injuries resulting from porcupine encounters. After adoption, the dog lived in NYC, spending summers and weekends in western Massachusetts, running freely on a large property with open fields and woodlands. Before presentation, the dog was healthy and had received routine vaccinations. Ticks were found by her owners on the surface of her fur but were not embedded.

Initial physical examination revealed a body weight of 19 kg, pyrexia (103.6°F), and sensitivity over the epaxial muscle region. Clinical pathology abnormalities included mild hypoalbuminemia (2.4 g/dL, range 2.7–3.9 g/dL), hyperglobulinemia (5.9 g/dL, range 2.4–4.8 g/dL), and lymphopenia (847/μL, range 1060–4950/μL). Fecal flotation test results were negative. An injection of meloxicam^a (dose not provided) was given SC, and metronidazole^b (20 mg/kg PO q12h) was prescribed for 8 days.

During the following week, the dog was reexamined for increasing lethargy, weakness, and pyrexia (103.4°F). Lyme quantitative C6 ELISA (Enzyme linked immunosorbent assay) was negative (<10 U/mL, range <30 U/mL)^c. The dog was seroreactive to *Anaplasma phagocytophilum* (1 : 400) and *Ehrlichia canis* (1 : 25) antigens

Abbreviations:

AMC	Animal Medical Center
FFPE	formalin-fixed paraffin embedded
GMS	Gomori's methenamine silver
ITS	intergenic transcribed spacer
NYC	New York City
PCR	polymerase chain reactions
ZN	Ziehl-Neelsen

by immunofluorescence antibody immunoassay, but was not seroreactive to *Rickettsia rickettsii*^c. Doxycycline^d (10 mg/kg PO q24h) and meloxicam^a (6 mg/kg PO q24h) were prescribed.

When reexamined 4 days later, the patient's rectal temperature was 100.2°F. Multiple, nonpainful, 1–2 cm diameter, raised cutaneous masses were observed on the left thigh and right ventral abdomen. Punch biopsies were obtained from the 2 ulcerated mass lesions and immediately fixed in formalin, after which the dog was prescribed metoclopramide^e (0.3 mg/kg PO q12h) and firocoxib^f (6 mg/kg PO q24h) and referred to the Animal Medical Center (AMC). Upon presentation to the AMC, the dog was hypothermic (95.9°) and eupneic at rest. Respiratory rate and effort increased with ambulation. Thoracic auscultation revealed focal, right-sided, fine, inspiratory crackles, and a sinus arrhythmia. Femoral pulse pressure was synchronous and hypokinetic. Neurological examination revealed lethargic mentation, decreased response to stimuli, and inconsistent conscious proprioceptive deficits. Gentle abdominal palpation elicited cranial and caudal discomfort. Venous blood gas findings were consistent with a metabolic acidosis. The dog was hypoxemic (SpO₂, 84%). Oscillometric blood pressure was 109/73 mmHg; however, systolic blood pressure dropped to 70 mmHg during hospitalization. Other laboratory abnormalities included neutrophilia (13.6 K/μL, range, 2.940–12.7 K/μL), thrombocytopenia (51 K/μL, range, 143–448 K/μL), increased alkaline phosphatase (587 U/L, range, 5–160 U/L), aspartate aminotransferase (76 U/L, range, 16–55 U/L) and creatine kinase (320 U/L, range, 10–200 U/L), hypoalbuminemia (1.1 g/dL, range, 2.7–3.9 g/dL), hyperglobulinemia (5.9 g/dL, range, 2.4–4.0 g/dL), hyperbilirubinemia (2.2 mg/dL, range, 0.0–0.3 mg/dL), (unconjugated 1.2 mg/dL, range, 0.0–0.2 mg/dL, conjugated 1.0 mg/dL, range, 0.0–0.1 mg/dL), azotemia (blood urea nitrogen 168 mg/dL, range, 9–31 mg/dL; creatinine 1.9 mg/dL, range, 0.5–1.5 mg/dL), and hyponatremia (124.4 mmol/L, range 135.0–148.0 mmol/L). Thoracic radiographs revealed a diffuse, alveolar pulmonary pattern.

From the Department of Pathology, (Donovan); Department of Cardiology, The Animal Medical Center, New York, NY (Fox); Department of Clinical Sciences, Intracellular Pathogens Research Laboratory, Center for Comparative Medicine and Translational Research, College of Veterinary Medicine, North Carolina State University, Raleigh, NC (Balakrishnan, Breitschwerdt); University of Minnesota Imaging Center, Minneapolis, MN (Ericson); and the The Animal Medical Center, New York, NY (Hooker).

Corresponding author: T. Donovan, Department of Pathology, The Animal Medical Center, 510 East 62nd St. New York, NY 10065; e-mail: Taryn.Donovan@amcn.org.

Submitted January 11, 2016; Revised September 21, 2016; Accepted October 18, 2016.

Copyright © 2016 The Authors. *Journal of Veterinary Internal Medicine* published by Wiley Periodicals, Inc. on behalf of the American College of Veterinary Internal Medicine.

This is an open access article under the terms of the Creative Commons Attribution-NonCommercial License, which permits use, distribution and reproduction in any medium, provided the original work is properly cited and is not used for commercial purposes.

DOI: 10.1111/jvim.14609

Abbreviated abdominal and thoracic ultrasound examinations detected pleural, pericardial, and peritoneal effusions. Fluid removed via abdominocentesis on 2 attempts revealed clotting blood (PCV/TS 13/5.6) and nonclotting serosanguinous fluid (PCV 3%). Cytologic evaluation of the serosanguinous fluid identified erythrocytes, few neutrophils, and band neutrophils. Punch biopsy results revealed pyogranulomatous, necrotizing dermatitis, and panniculitis. Special stains for fungus (Gomori's methenamine silver, GMS) and acid fast bacteria (Ziehl-Neelsen, ZN) were negative. Despite supportive emergency treatment, vital signs declined. The patient's owners elected euthanasia and granted permission for necropsy, 16 days after initial medical examination. The postmortem interval was between 6 and 12 hours.

Gross Pathology

Approximately 350 mL of serosanguinous, pleural effusion and 60 mL of serosanguinous, pericardial effusion intermixed with fibrin were present. The heart was mildly enlarged (1.14% of body weight). Visible from the epicardium of all 4 cardiac chambers was a miliary pattern created by myriad pinpoint, multifocal to coalescing, tan to white nodular foci (Fig 1) which extended into the myocardium and endocardium. The left atrioventricular valve leaflets were thickened at the distal aspect without chordae tendineae involvement, consistent with grade II myxomatous valvular degeneration.¹ The lungs were diffusely dark red, rubbery to firm, and upon sectioning, exuded serosanguinous fluid. Sections from the right middle and right cranial lung lobes sank in formalin, suggesting cellular infiltration. The abdomen contained 30 mL of serosanguinous effusion and small amounts of clotted blood (the latter presumed to be secondary to abdominocentesis). The kidneys were bilaterally enlarged and contained myriad,

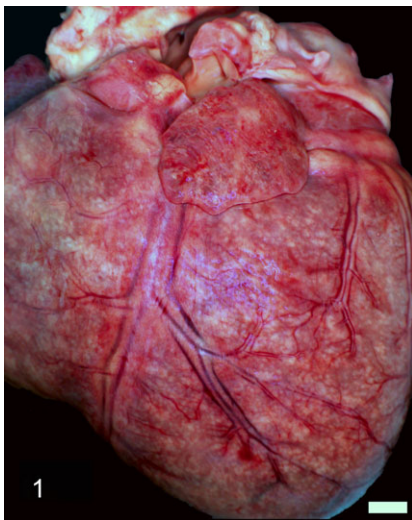


Fig 1. Heart, dog. Myriad, multifocal to coalescing white to tan nodular foci are visible from the epicardium of the right and left ventricles and atria. Bar = 5 mm.

multifocal to coalescing, tan to light red, irregular, nodular foci, ranging from pinpoint to 1.0 cm in diameter (Figs 2, 3). Marked hepatomegaly was present (5.5% body weight), and the liver had a diffusely enhanced reticular pattern with plaques of fibrin over the capsule and diaphragm. A single porcupine quill was encased in the proximal right lateral liver lobe with no grossly apparent tissue reaction. Lymphadenomegaly was observed including the retropharyngeal, mandibular, sternal, renal, tracheobronchial, pancreaticoduodenal, and mesenteric lymph nodes.

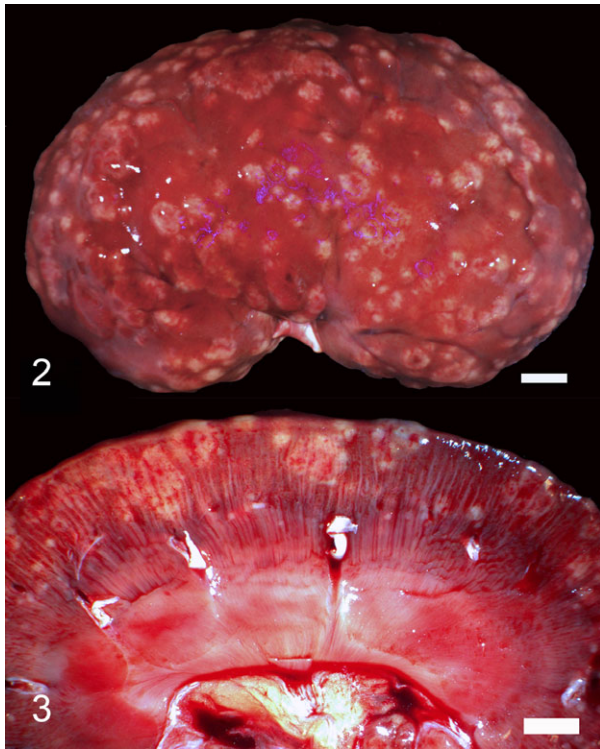
Microscopic Findings

Impression smears of the kidney and heart revealed large numbers of neutrophils and macrophages, with fewer lymphocytes and plasma cells. Bacteria were not observed. Cardiac histopathology revealed multifocal to coalescing, transmural, severe, pyogranulomatous, lymphoplasmacytic myocarditis, epicarditis, and endocarditis (pancarditis) with regional cardiomyocyte degeneration and necrosis (Fig 4). There was variable inflammation in the right and left atrioventricular valves and pulmonic and aortic valves. Rare, granulomatous, pyogranulomatous, or lymphoplasmacytic vasculitis was noted. The kidneys contained extensive, multifocal to coalescing, pyogranulomatous, tubulointerstitial nephritis with degeneration, necrosis and regeneration of tubules in areas of inflammation (Fig 5). In the lungs, neutrophilic, pyogranulomatous, and lymphoplasmacytic interstitial pneumonia was present in all lobes, with necrosis, fibrin exudation, edema, alveolar histiocytosis, arteritis, periarteritis, and mild type II pneumocyte hyperplasia. Pyogranulomatous and lymphoplasmacytic arteritis and periarteritis were prominent in lung samples (Fig 6). Chronic, passive hepatic congestion was observed. Pyogranulomatous meningitis, encephalitis, anterior uveitis, scleritis, lymphadenitis, tracheitis, peritracheitis, cystitis, capsular splenitis, and mediastinal periarteritis were also noted. In addition to mild lymphadenitis, enlarged lymph nodes exhibited changes consistent with reactive hyperplasia. The adrenal glands did not exhibit adrenalitis or atrophy.

Special stains for fungus (GMS), acid fast bacteria (ZN and Fite faraco), protozoa (periodic acid-Schiff), and bacteria (Brown and Brenn, Warthin-Starry) were negative on the heart, kidney, and lungs. Warthin-Starry silver stains contained abundant artifact, which hindered interpretation.

Polymerase Chain Reactions (PCR) and DNA Sequencing

DNA was extracted from fresh-frozen canine heart, formalin-fixed, paraffin-embedded (FFPE) heart, kidney, lung, lymph node, trachea, urinary bladder, adrenal glands, brain and eye tissues with DNeasy Blood and Tissue Kit^g according to the manufacturer's instructions. Elution buffer was used as a reagent control with each set of DNA extractions. DNA concentration and purity were determined with a spectrophotometer.^h Extracted



Figs 2 and 3. Kidney, dog. Visible from the renal cortex are dozens of multifocal to coalescing, tan nodular foci, which range from pinpoint to 1 cm in diameter. Bar = 5 mm.

DNA was stored at -20°C . *Bartonella* genus and *B. koehlerae* species-specific PCRs were performed with primers designed to amplify the 16–23S intergenic transcribed spacer (ITS) region.² *Bartonella* DNA was amplified only from fresh heart tissue, whereas FFPE kidney, lung, lymph node, trachea, urinary bladder, adrenal glands, brain, and eye were PCR negative for *Bartonella* spp. By sequencing, *Bartonella henselae* San Antonio 2 (*BhSA2*) DNA amplified from fresh heart tissue shared 100% (444/444 base pairs) DNA sequence similarity with *BhSA2* (GenBank accession number AF369529.1).

Eubacterial PCR with pan oligonucleotide primers targeting the 16S rRNA gene was performed as described previously on FFPE heart, kidney, lung, lymph node, trachea, urinary bladder, adrenal glands, brain, and eye, respectively.³ Briefly, 25 μL reaction volume consisted of 10 μM forward (fD1-5-AGAGTTTGATCCTGGCTCA G-3; *Escherichia coli* spanning position 339–357) and reverse (rP2-5-ACGGCTACCTTGTTACGACTT-3; *E. coli* spanning position 519–536) primers, 5 μL template DNA and 12.5 μL of MyTaq master mix.¹ The thermocycling conditions included initial denaturation (94°C for 2 minutes) followed by 35 cycles of denaturation (94°C for 30 seconds), annealing (68°C for 30 seconds) extension (72°C for 1 minute), and final extension (72°C for 1 minute).³ None of the FFPE tissues tested were positive for pathogenic bacteria.

Scrolls from FFPE blocks of heart, kidney, and lung were submitted for PCR testing for canine circovirus, canine herpesvirus, canine adenovirus, *Blastomyces* spp.,

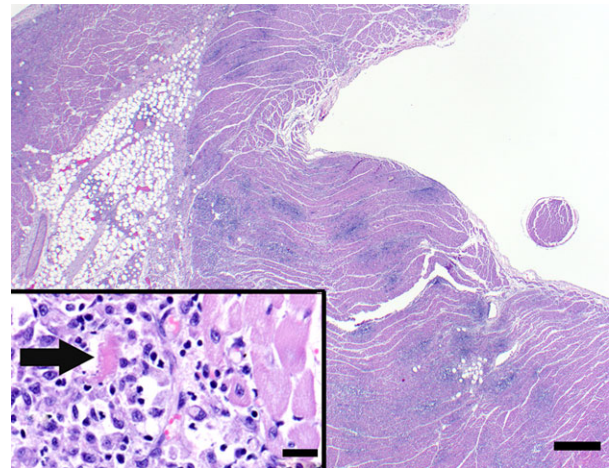


Fig 4. Heart, dog. Low magnification view of the right ventricle and atrium. Multifocal to coalescing regions of increased cellular density (pyogranulomatous inflammation) are visible in the epicardium, myocardium, and endocardium, consistent with pancarditis. H&E. Bar = 500 μm . Inset. Higher magnification view of pyogranulomatous inflammation within the left ventricular myocardium. Neutrophils and macrophages are observed throughout the myocardial interstitium, separating cardiomyocytes. Regional cardiomyocytes undergo degeneration and necrosis (arrow), with sarcoplasmic hypereosinophilia, loss of visible striations, and karyorrhectic debris. HE. Bar = 20 μm .

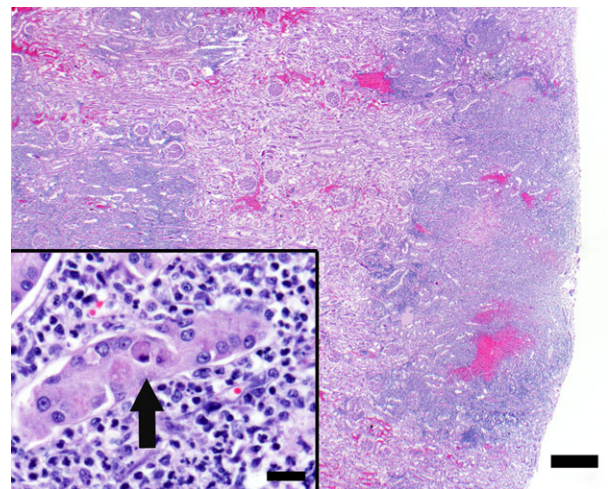


Fig 5. Kidney, dog. Low magnification view of a section of kidney. Large regions of multifocal to coalescing hypercellularity are present within the cortex, representing pyogranulomatous nephritis. HE. Bar = 500 μm . Inset. Higher magnification view of a section of kidney. Neutrophils and macrophages are observed throughout the interstitium. The renal tubular epithelial cells undergo degeneration, necrosis, and regeneration, with cytoplasmic hypereosinophilia, nuclear pyknosis, karyolysis (arrow), and crowding of tubular epithelial nuclei. HE. Bar = 20 μm .

Histoplasma spp., *Coccidiomyces* spp., *Cryptococcus* spp., *Sporothrix* spp., *Trichophyton* spp.,¹ *Borrelia burgdorferi*, *Anaplasma* spp., *Rickettsia* spp., *Ehrlichia* spp., and *Bartonella*.^k All of these PCR results were negative.

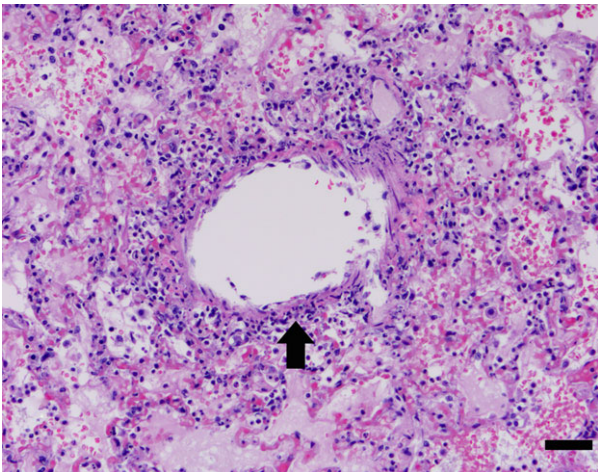


Fig 6. Lung, dog. Photomicrograph of a section of lung. The interstitium is hypercellular, containing mixed inflammatory infiltrates, including neutrophils, macrophages, lymphocytes, and plasma cells. Hemorrhage, edema, and alveolar macrophages are present within the alveolar spaces. Inflammatory cells extend into the wall of an arteriole (arteritis, arrow). HE. Bar = 50 μ m.

Multiphoton Laser Scanning Microscopy

Deparaffinized floating sections (50 μ m) of the dog's heart were immunostained with a mouse anti-*B. henselae* antibody¹ at 1 : 100 dilution and a secondary antibody donkey anti-mouse conjugated to Alexa 488^m at 1 : 400 dilution by previously published protocols.⁴ Thirteen 0.45- μ m optical sections (total Z projection = 5.85 μ m) were captured by multiphoton laser scanning microscopy (Nikon A1RMP—University of Minnesota Imaging Center) with a Nikon Plan Apo LWD25X 1.10W DICN2, Melville, NY 11747, USA objective and electronic zoom = 2). *Bartonella henselae* organisms (green) were visualized in the myocardium (Fig 7). These organisms were frequently amorphous and nonlinear, interpreted to be present in clumps or clusters. With multiphoton microscopy, we were able to clearly separate the epifluorescent signal contribution of endogenous lipofuscin (red channel) from the *B. henselae* immunoreactivity (green channel).^{5,6} Heart tissue incubated with only the secondary antibody (antibody control) showed no signal in the green channel (data not shown). A negative control on normal canine heart tissue was not performed.

Discussion

This report describes pyogranulomatous myocarditis, epicarditis, and endocarditis (pancarditis) in a dog infected with *B. henselae* SA2. *Bartonella henselae* organisms were documented in the heart using *Bartonella* genus-specific 16–23S ITS elements PCR amplification from fresh heart tissue. *Bartonella henselae* organisms were visualized with immunoreactivity with multiphoton laser confocal microscopy, a novel technique which has not been previously described for identification of *Bartonella* in canine tissue. This case was

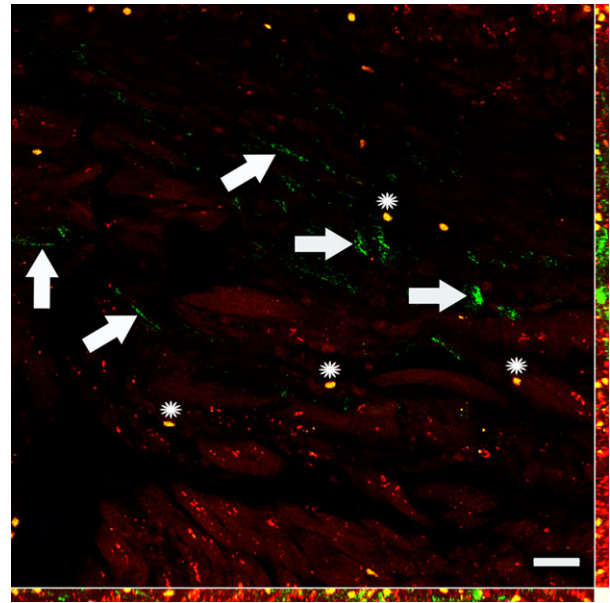


Fig 7. Multiphoton laser scanning microscopy demonstrates *Bartonella henselae* immunoreactivity (green, large white arrows) in the myocardium. Fluorescence excitation was at 970 nm, and emission data were collected at 535 nm to capture the green channel epifluorescence and 620 nm to capture red channel epifluorescence. Under these image capture settings, there is no contribution by lipofuscin in the green channel. Erythrocytes (asterisks) appear yellow due hemoglobin autofluorescence in both the red and green emission channels (535 and 609 nm). Inflammatory cells do not autofluoresce (not visible). Image is a single in-focus projection of 22 0.45- μ m-thick optical z-sections captured with an Apo LWD 25X 1.10W DIC N2 objective on a Nikon A1RMP multiphoton microscope in the University Imaging Centers at the University of Minnesota. Orthogonal or right angle data, YZ and XZ projections, on the right and bottom margins of the image (respectively) display the 3-dimensional data in a 2-dimensional format. Scale bar = 20 μ m.

notable for its wide-ranging, multi-organ pathology, particularly pyogranulomatous pancarditis, nephritis, and interstitial pneumonia with tricavitary effusion. We were unable to document coinfection with other infectious organisms. Diagnostic investigations in this case were limited by the lack of bacterial culture or virus isolation on fresh tissues at the time of necropsy. Collectively, findings were suggestive of bacteremia; however, neither *Bartonella* spp. nor any other infectious organisms could be identified in multiple additional organs tested by PCR, including 16S rDNA eubacterial PCR for fastidious and nonfastidious bacteria. We were unable to demonstrate the colocalization of *Bartonella* organisms in the inflammatory foci with traditional immunohistochemistry despite the immune reaction demonstrated with confocal microscopy. Possible explanations for these discrepancies are discussed.

Bartonella henselae has important one health implications and has been associated with a wide spectrum of clinical disease syndromes in dogs and humans.^{7–18} *Bartonella* spp. are Gram-negative, alpha-proteobacteria implicated as a cause of culture-negative endocarditis,

arrhythmias, myocarditis, and sudden death in animals and humans.⁸ This fastidious, intracellular, vasculotropic bacterium is commonly referred to as a stealth pathogen and characteristically causes persistent intravascular infections.^{9,10} *Bartonella* spp. may cause a chronic relapsing bacteremia among reservoir hosts and resultant opportunistic infections in nonreservoir hosts.^{9–17} Due to *Bartonella*'s ability to cause persistent infection within numerous cell types, demonstration of causation is often challenging and requires a high index of suspicion.¹⁷

Additional, follow-up PCR performed on FFPE tissues from multiple organs was negative. The FFPE heart samples were obtained from a different location than the fresh cardiac tissue. Pathogen DNA amplification may be affected by the size of the tissue placed in formalin, the type of tissue, and the duration of formalin fixation before embedding. DNA degradation during formalin fixation has been well documented,^{7,19} especially in detecting *B. henselae* in splenic⁷ and skin tissues (N. Balakrishnan, Perdergraft JS, Kolluru S, Lappin M, Breitschwerdt EB, unpublished data). Additionally, low numbers of *Bartonella* within some of the inflammatory lesions or the history of antibiotic treatment may have mitigated the ability to detect bacterial pathogens in the other organs tested. In this patient, *Bartonella* may have survived intact within the heart due to persistent intracellular or intravascular infection and periodic dissemination to other tissues.¹³ *Bartonella* has been shown to have higher bacterial loads in the heart and lymph node as compared with other parenchymal tissues,¹⁴ which may help to explain the lack of *Bartonella* positivity in other tissues tested.¹⁴

The cardiac gross and histologic findings of this case are similar to 2 previously reported feline cases of pyogranulomatous myocarditis and diaphragmatic myositis, in which *Bartonella* were demonstrated with Warthin-Starry and Steiner silver stains, *Bartonella* immunohistochemistry, and PCR.² Pancardial involvement was not observed in the feline cases.² In this case, we were unable to document the presence of *Bartonella* organisms in 5- μ m-thick heart sections via Warthin-Starry silver stains and *Bartonella* immunohistochemistry. Multiphoton confocal microscopy uses 50- μ m-thick floating sections and multiple *Bartonella* gene targets, resulting in an increased sensitivity for detecting low copy numbers of *Bartonella* spp. as previously documented.^{20,21} Apparent clumping or clustering of the bacteria is demonstrated by the confocal microscopy image. These results are similar to the aforementioned case series of feline myocardial *Bartonella* infections,² although bacterial visualization was achieved with different techniques (silver stains and immunohistochemistry). A possible explanation for the clusters is aggregation of bacteria within a biofilm matrix; however, there is no evidence to substantiate this possibility. Unfortunately, the exact location of the bacteria (intracellular or extracellular) could not be determined.

With the current case, myocarditis attributed to *B. henselae* has now been reported in 3 mammalian genera including cats, dogs, and humans.^{2,8,13,15,17,18,22}

Myocarditis was described in 2 dogs seroreactive to *Bartonella vinsonii* subspecies *berkhoffii* antigens, with PCR amplification in 1 dog; however, *Bartonella* bacteria were not visualized within the myocardium. Both of these dogs had concurrent endocarditis with vegetative lesions.⁸ The cause for the relatively few reported cases of *Bartonella* myocarditis is unknown and may be attributable to a truly low incidence, difficulty in establishing a definitive diagnosis, occurrence of occult disease, or unfamiliarity with this agent as a differential diagnosis.¹⁷

Pyogranulomatous inflammation involving a single organ or multiple tissues occurs with *B. henselae* in humans^{14,16,18,23,24}, cats,^{2,17} and dogs.^{14,15,18,22,25–31} Natural infection with *B. henselae* or *B. vinsonii* subsp *berkhoffii* in dogs has been correlated with granulomatous hepatitis, rhinitis, sialoadenitis, mediastinitis, polyarthritides, lymphadenitis, uveitis, meningitis, encephalitis, and panniculitis,^{18,25–31} the latter 5 of which were observed in this case.

Coinfections might contribute to complex interactions among microbial populations, aberrant host immune response, and atypical disease manifestations as compared to single pathogen infections. The dog in the present report was seroreactive to *A. phagocytophilum* and *E. canis* antigens. Numerous bacterial, fungal, and rickettsial PCR analyses of multiple FFPE tissues were negative. In a reported series of 12 dogs with cardiac arrhythmias, endocarditis, myocarditis, syncope, conduction defects, or sudden death, 11 were seroreactive to *B. vinsonii* subspecies *berkhoffii* antigens, and 7 were coinfecting with other tick-transmitted pathogens including *E. canis*, *Babesia canis*, *Babesia gibsonii*, or spotted fever group *Rickettsiae*.⁸ Given the breed (American Pitbull terrier) in the present report, predisposition for *Babesia* infection is possible,³² although no hemoparasites were identified with CBC evaluation. A recent study demonstrated *B. burgdorferi* antigen using immunohistochemistry in 10 Boxer puppies with pyogranulomatous myocarditis.³³ In this case, both serological testing and PCR were negative for *Borrelia* spp., although immunohistochemistry was not performed. Differential diagnoses for cardiopulmonary vasculitis in the present case include systemic bacterial, rickettsial, fungal or viral infections, autoimmune diseases; food or drug reaction; and uremia.³⁴ Interestingly, although vasculitis is not a recognized sequel to *Bartonella* infection in dogs, *B. henselae* has been implicated in reported cases of human vasculitis.¹⁷

The source of infection in this case was undetermined. As the dog had a history of tick exposure, tick transmission is plausible. Alternatively, the wound of unknown origin, exposure to fleas, or other arthropod vectors may have been the source of infection. Although cat fleas (*Ctenocephalides felis*) are considered the primary vector, *B. henselae* DNA has also been amplified from other arthropods, which might indicate more ecologically diverse modes of transmission.^{35–38}

In conclusion, this report describes extensive pyogranulomatous inflammation in a dog, including severe cardiac involvement. Clusters of *B. henselae* were demonstrated within the myocardium by immunoreactivity with

multiphoton laser scanning confocal microscopy. It must be noted that the conclusions of this study are limited in determining whether *Bartonella* alone or in combination with other organisms were the cause of the disseminated inflammatory processes in this patient, as additional immunohistochemical and molecular tests failed to identify *Bartonella* or other infectious organisms within the inflamed FFPE tissues. Future studies are required to characterize the relationship between the host and *Bartonella* virulence for improved understanding of patterns of disease manifestation and optimization of diagnosis and treatment.

Footnotes

- ^a Meloxicam Metacam, Norbrook Laboratories, Ltd., Lenexa, KS
^b Metronidazole Flagyl, Teva Pharmaceuticals, NJ
^c IDEXX Laboratories, Inc., Westbrook, ME
^d Doxycycline Vibramycin, Pfizer Pharmaceuticals, New York, NY
^e Metoclopramide Reglan, Teva Pharmaceuticals, Fairfield, NJ
^f Firocoxib Previcox, Merial Ltd., Duluth, GA
^g Qiagen, Valencia, CA
^h Nanodrop, Wilmington, DE
ⁱ Bioline, Taunton, MA USA
^j IDEXX Laboratories Inc, West Sacramento, CA
^k NCSU-CVM Vector Borne Diseases Diagnostic Laboratory, Raleigh, NC
^l Abcam, Cambridge, MA
^m Jackson ImmunoResearch, West Grove, PA

Acknowledgments

The authors acknowledge Dr. Keith Linder for performing immunohistochemistry; Ms. Brittany Thomas and Dr. Ricardo Maggi in the NCSU-CVM Vector Borne Diseases Diagnostic Laboratory for PCR testing; Dr. Christian M. Leutenegger and Dr. Marko Estrada of IDEXX Laboratories, Inc., West Sacramento, CA 95605 for performing numerous PCR analyses; Ms. Amanda Ramkissoon, Ms. Nanette Ramkissoon, Ms Iveta Simanska, and IDEXX Laboratories, Inc., Grafton, MA, 01536 for data acquisition, slide preparation, and special stains; Dr. Alexandre Rousseau for review of clinical data and Ms. Barbara Hegarty for review of the manuscript.

Grant support: The author disclosed receipt of the following financial support for the research, authorship, or publication of this article: The authors received financial support from the Schiff Foundation and the Caspary Institute of the Animal Medical Center and the Vector Borne Diseases Research Foundation Account at North Carolina State University College of Veterinary Medicine to support clinical and laboratory diagnostic testing.

Conflict of Interest Declaration: The authors declared no potential conflict of interest with respect to the research, authorship, or publication of this article.

Off-label Antimicrobial Declaration: Authors declare no off-label use of antimicrobials.

References

- Pomerance A, Whitney JC. Heart valve changes common to man and dog: A comparative study. *Cardiovasc Res* 1970;4:61–66.
- Varanat M, Broadhurst J, Linder KE, et al. Identification of *Bartonella henselae* in 2 cats with pyogranulomatous myocarditis and diaphragmatic myositis. *Vet Pathol* 2012;49:608–611.
- Balakrishnan N, Alexander K, Keene B, et al. Successful treatment of mitral valve endocarditis in a dog associated with *Actinomyces canis*-like infection. *J Vet Cardiol* 2016;18:271–277.
- Wacnik PW, Baker CM, Herron MJ, et al. Tumor-induced mechanical hyperalgesia involves CGRP receptors and altered innervation and vascularization of DsRed2 fluorescent hindpaw tumors. *Pain* 2005;115:95–106.
- Zipfel WR, Williams RM, Christie R, et al. Live tissue intrinsic emission microscopy using multiphoton-excited native fluorescence and second harmonic generation. *Proc Natl Acad Sci USA* 2003;100:7075–7080.
- Li D, Zheng W, Zeng Y, et al. Two-photon excited hemoglobin fluorescence provides contrast mechanism for label-free imaging of microvasculature in vivo. *Opt Lett* 2011;36:834–846.
- Balakrishnan N, Jawanda JS, Miller MB, Breitschwerdt EB. *Bartonella henselae* in a man with hypergammaglobulinaemia, splenomegaly and polyclonal plasmacytosis. *J Med Microbiol* 2013;62:338–341.
- Breitschwerdt EB, Atkins CE, Brown TT, et al. *Bartonella vinsonii* subsp. *berkhoffii* and related members of the alpha subdivision of the proteobacteria in dogs with cardiac arrhythmias, endocarditis or myocarditis. *J Clin Microbiol* 1999;37:3618–3626.
- Breitschwerdt EB, Linder KL, Day MJ, et al. Kochs postulates and the pathogenesis of comparative infectious disease causation associated with *Bartonella* species. *J Comp Pathol* 2013;148:115–125.
- Merrell DS, Falkow S. Frontal and stealth attack strategies in microbial pathogenesis. *Nature* 2004;430:250–256.
- Chomel BB, Kasten RW, Williams C, et al. *Bartonella* endocarditis: A pathology shared by animal reservoirs and patients. *Ann N Y Acad Sci* 2009;1166:120–126.
- Pesavento PA, Chomel BB, Kasten RW, et al. Pathology of *Bartonella* endocarditis in six dogs. *Vet Pathol* 2005;42:370–373.
- Breitschwerdt EB, Kordick DL. *Bartonella* infection in animals: Carriership, reservoir potential, pathogenicity and zoonotic potential for human infection. *Clin Microbiol Rev* 2000;13:428–438.
- Breitschwerdt EB, Maggi RG, Chomel BB, Lappin MR. Bartonellosis: An emerging infectious disease of zoonotic importance to animals and human beings. *J Vet Emerg Crit Care* 2010;20:8–30.
- Chomel BB, Boulouis HJ, Maruyama S, Breitschwerdt EB. *Bartonella* spp. in pets and effect on human health. *Emerg Infect Dis* 2006;12:389–394.
- Mazur-Melewska K, Mania A, Kemnitz P, et al. Cat-scratch disease: A wide spectrum of clinical pictures. *Postepy Dermatol Alergol* 2015;32:216–220.
- Breitschwerdt EB, Kordick DL. *Bartonella* species and vascular pathology. In: Gavins FNE, Stokes KY, eds. *Vascular Responses to Pathogens*. London: Elsevier; 2016:61–71.
- Breitschwerdt EB, Maggi RG. Comparative medical features of canine and human bartonellosis. *Clin Microbiol Infect* 2009;15(Suppl 2):106–107.
- Koshiha M, Ogawa K, Hamazaki S, et al. The effect of formalin fixation on DNA and the extraction of high molecular weight DNA from fixed and embedded tissues. *Pathol Res Pract* 1993;189:66–72.
- Pultorak EL, Linder K, Maggi RG, et al. Prevalence of *Bartonella* spp. in canine cutaneous histiocytoma. *J Comp Pathol* 2015;153:14–21.

21. Maggi RG, Ericson M, Mascarelli PE, et al. *Bartonella henselae* bacteremia in a mother and son potentially associated with tick exposure. *Parasit Vectors* 2013;15:101.
22. Saunders GK, Monroe WE. Systemic granulomatous disease and sialometaplasia in a dog with *Bartonella* infection. *Vet Pathol* 2006;43:391–392.
23. VanderHeyen TR, Yong SL, Breitschwerdt EB, et al. Granulomatous hepatitis due to *Bartonella henselae* infection in an immunocompetent patient. *BMC Infect Dis* 2012;12:17.
24. Gerber JE, Johnson JE, Scott MA, Madhusudhan KT. Fatal meningitis and encephalitis due to *Bartonella henselae* bacteria. *J Forensic Sci* 2002;47:640–644.
25. Drut A, Bublot I, Breitschwerdt EB, et al. Comparative microbiological features of *Bartonella henselae* infection in a dog with fever of unknown origin and granulomatous lymphadenitis. *Med Microbiol Immunol* 2014;203:85–91.
26. Tucker MD, Sellon RK, Tucker RL, et al. Bilateral mandibular pyogranulomatous lymphadenitis and pulmonary nodules in a dog with *Bartonella henselae* bacteremia. *Can Vet J* 2014;55:970–974.
27. Gillespie TN, Washabau RJ, Goldschmidt MH, et al. Detection of *Bartonella henselae* and *Bartonella clarridgeiae* DNA in hepatic specimens from two dogs with hepatic disease. *J Am Vet Med Assoc* 2003;222:47–51.
28. Mellor PJ, Fetz K, Maggi RG, et al. Alpha1-proteinase inhibitor deficiency and *Bartonella* infection in association with panniculitis, polyarthritis, and meningitis in a dog. *J Vet Intern Med* 2006;20:1023–1028.
29. Morales SC, Breitschwerdt EB, Washabau RJ, et al. Detection of *Bartonella henselae* DNA in two dogs with pyogranulomatous lymphadenitis. *J Am Vet Med Assoc* 2007;230:681–685.
30. Pappalardo BL, Brown T, Gookin JL, et al. Granulomatous disease associated with *Bartonella* infection in 2 dogs. *J Vet Intern Med* 2000;14:37–42.
31. Rossi MA, Balakrishnan N, Linder KE, et al. Concurrent *Bartonella henselae* infection in a dog with panniculitis and owner with ulcerated nodular skin lesions. *Vet Dermatol* 2015;26:60–63.
32. Jefferies R, Ryan UM, Jardine J, et al. Blood, bull terriers and babesiosis: Further evidence for direct transmission of *Babesia gibsoni* in dogs. *Aust Vet J* 2007;85:459–463.
33. Detmer SE, Bouljihad M, Hayden DW, et al. Fatal pyogranulomatous myocarditis in 10 boxer puppies. *J Vet Diagn Invest* 2016;28:144–149.
34. Maxie MG, Robinson WF. Cardiovascular system. In: Maxie MG, ed. *Pathology of Domestic Animals*, 5th ed, Vol. 3. Edinburgh: Elsevier; 2007:1–107.
35. Billeter SA, Levy MG, Chomel BB, Breitschwerdt EB. Vector transmission of *Bartonella* species with emphasis on the potential for the tick transmission. *Med Vet Entomol* 2008;22:1–15.
36. Dietrich F, Schmidgen T, Maggi RG, et al. Prevalence of *Bartonella henselae* and *Borrelia burgdorferi* sensu lato DNA in *Ixodes ricinus* ticks in Europe. *Appl Environ Microbiol* 2010;76:1395–1398.
37. Mascarelli PE, Maggi RG, Hopkins S, et al. *Bartonella henselae* infection in a family experiencing neurological and neurocognitive abnormalities after woodlouse hunter spider bites. *Parasit Vectors* 2013;6:98.
38. Bradley JB, Mascarelli PE, Trull CL, et al. *Bartonella henselae* infection in an owner and two Papillon dogs exposed to tropical rat mites (*Ornithonyssus bacoti*). *Vector Borne Zoonotic Dis* 2014;14:703–709.